Korea-Australia Rheology Journal
Vol. 21, No. 4, December 2009 pp. 289-297

Optimum shape and process design of single rotor equipment for its mixing performance using finite volume method

Naksoo Kim* and Jaeyeol Lee
Dept. of Mechanical Engineering, Sogang University, 1, Sinsu-dong, Mapo-gu, Seoul 121-742, Korea
(Received January 5, 2009; final version received November 17, 2009)

Abstract

We numerically analyzed flow characteristics of the polymer melt in the screw equipment using a proper modeling and investigated design parameters which have influence on the mixing performance as the capability of the screw equipment. We considered the non-Newtonian and non-isothermal flow in a single rotor equipment to investigate the mixing performance with respect to screw dimensions as shape parameter of the single rotor equipment and screw speed as process parameter. We used Bird-Carreau-Yasuda model as a viscous model of the polymer melt and the particle tracking method to investigate the mixing performance in the screw equipment and considered four mixing performance indexes: residence time distribution, deformation rate, total strain and particle standard deviation as a new mixing performance index. We compared these indexes to determine design parameters and object function. On basis of the analysis results, we carried out the optimal design by using the response surface method and design of experiments. In conclusion, the differences of results between the optimal value and numerical analysis are about 5.0%.

Keywords : single rotor equipment, mixing performance, design of the experiments, response surface method, optimum design

1. Introduction

Optimal design of screw extrusion can enhance the efficiency of mixing performance between nano-scaled clay particles and polymer melt. However, there are few studies about the optimal design of screw extrusion. Furthermore, most companies design and operate a screw extruder on the basis of not systematic knowledge but their experience accumulated at actual field. Therefore, it is essential that we numerically analyze flow characteristics of the polymer melt in the screw extruder using a proper modeling and investigate design parameters which have influence on the mixing performance as the capability of the screw extruder.

Griffith (1962) studied the fully developed flow of incompressible fluid using Power-law model as a viscous model of the polymer melt. Fenner (1977) analyzed the flow characteristics in a screw extruder for a variation of the temperature with respect to the length of the channel. Also, Karwe and Jaluria (1990) carried out a study about heat transfer of non-Newtonian fluids. On the other hand, Sastrohartono *et al.* (1994) performed a flow analysis of polymer melt by using marching scheme. Furthermore, they compared numerical results to with experimental results. Kwon *et al.* (1993) studied kinematics and deformation characteristics and Kim and Kwon (1996a, 1996b) studied single-screw extrusion process to enhance the mixing performances.

Shearer and Tzoganakis (2000) studied the interfacial reaction between polymer melts using a microscopic probe to analyze the mixing performance. Also, Bakalis and Karwe (2002) carried out an experimental study to compare the velocity and mass flux distributions in the nip and translation regions. Bravo *et al.* (2004) also studied the mixing performance of twin screw extruder. Syrjala (1999) carried out a research on the three dimensional fluid flow in the conveying section of single screw extruder using the marching scheme which contiguously solved the equation given in the perpendicular section to down channel. The validity of the methodology has been verified later with experiment data (Syrjala, 2000).

Also, there are many studies about the numerical analysis for the flow characteristics of the polymer melt. Kwag *et al.* (2001) carried out the flow and thermal analysis for the three dimensional non-Newtonian fluid in a screw extruder. They used the commercial code, STAR-CD for FVM (finite volume method). Ahmad and Jean-Robert (2005) modeled a screw extruder without geometry approximation. They numerically analyzed the non-isothermal and steady-state flow in the three-dimension by using FVM. On the other hand, Bravo and Hrymak (2000) and Ishikawa *et al.* (2000) performed research studies that

*Corresponding author: nskim@sogang.ac.kr

investigated kneading elements of a co-rotating twin screw extruder. Yoshinaga et al. (2000) carried out a study about kneading elements of a co-rotating screw extruder using FEM (finite element method). Furthermore, they used the marker tracking method to estimate the mixing performance of the screw extruder. Ishikawa and Amano (2002) studied the mixing performance with respect to the various shapes of the screws. Also, Linjie *et al.* (2005) used a commercial code, FLUENT to analyze polymerization reaction degree with respect to process conditions.

In a preceding study, Ye *et al.* (2005) performed a research about polymer extrusion processes with the FEM using a 4-step fractional method. Also, Kim *et al.* (2006a, 2006b) studied about the flow characteristics and mixing performance with respect to the pitch as shape parameter of screw extruder and screw speed as process condition. The Carreau-Yasuda model and FVM are considered for the numerical analysis in these studies.

In this study, we properly modeled a single rotor equipment without approximating geometry and investigated design parameters which have influence on the mixing performance. Furthermore, we compared four mixing performance indexes to select an object function of the optimal design for the screw equipment. Ultimately, we presented a methodology for the optimal design by using RSM (response surface method) and DOE (design of experiments) to obtain the highest mixing performance in the screw equipment. For simplicity, the current study didn't consider the Booy's equation to the screw root geometry.

2. Theory

2.1. Governing equations

In general, the polymer melt is a non-Newtonian fluid. Its flow characteristics are incompressible and laminar. To express these flow characteristics in the Cartesian coordinate system, the continuity and momentum equations (Kim *et al.*, 2006a) are given as follows:

$$\frac{\partial\rho}{\partial t}+\frac{\partial}{\partial x_j}(\rho u_j)=s_m, \tag{1}$$

$$\frac{\partial(\rho u_i)}{\partial t}+\frac{\partial}{\partial x_j}(\rho u_j u_i-\tau_{ij})=-\frac{\partial p}{\partial x_i}+s_i, \tag{2}$$

$$\frac{\partial(\rho h)}{\partial t}+\frac{\partial}{\partial x_j}(\rho h u_j+F_{h,j})=\frac{\partial p}{\partial t}+u_j\frac{\partial p}{\partial x_j}+\tau_{ij}\frac{\partial u_i}{\partial x_j}+s_h. \tag{3}$$

These equations are calculated using the PISO (pressure implicit with splitting of operators) algorithm in FVM. The flux term is solved by the upwind scheme. The shear stress is expressed by the following constitutive law.

$$\tau_{ij}=2\mu s_{ij}-\frac{2}{3}\mu\frac{\partial u_k}{\partial x_k}\delta_{ij},$$

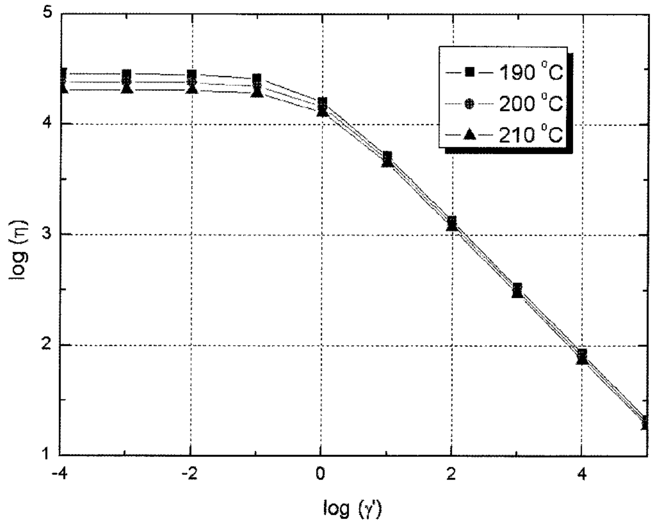

Fig. 1. Bird-Carreau-Yasuda model for HDPE.

$$\text{where } s_{ij}=\frac{1}{2}\left(\frac{\partial u_i}{\partial x_j}+\frac{\partial u_j}{\partial x_i}\right). \tag{4}$$

2.2. Bird-Carreau-Yasuda model

The Bird-Carreau-Yasuda model is considered as a viscous model of the polymer melt. This model is the modified Carreau-Yasuda model, which includes temperature dependence and is written as follows:

$$\mu=\frac{k_1 a_T}{[1+k_2\dot{\gamma}a_T]^{k3}},\ \text{where } a_T=exp\left[\frac{E_o}{R}\left(\frac{1}{T}-\frac{1}{T_o}\right)\right] \text{ and}$$

$$\dot{\gamma}=\sqrt{\frac{1}{2}(s_{ij}s_{ij}-s_{ii}s_{jj})}. \tag{5}$$

As shown in equation (5), the Bird-Carreau-Yasuda model includes both the deformation rate ($\dot{\gamma}$) and shift (a_T) as a function of temperature. This viscous model is transformed to a user subroutine in the FVM calculation.

In this study, we considered HDPE (high density polyethylene) as the polymer melt. Fig. 1 shows the Bird-Carreau-Yasuda model of HDPE with respect the temperature and deformation rate. Furthermore, constant values of this model and properties of HDPE are shown in Table 1 (Osswald, 2006).

2.3. Design of experiments using the orthogonal array table

DOE is defined as a plan of experiments that includes the method of setting up an experiment about a problem, method of data collection and method of obtaining the maximum amount of information in the minimum number of experiments based on statistical data analysis (Lim *et al.*, 1999). In other words, using DOE requires the selection of parameters about a problem, selection of an experimental method, decision on the experiment order and

Table 1. Properties of HDPE (Osswald and Menges, 2007)

Viscous model	
$k1$ [Pa sec]	24198
$k2$ [sec]	1.38
k_3	0.60
Eo/R [°C]	3350.5
To [°C]	200
Physical properties	
Thermal conductivity [W/m°C^{-1}]	0.63
Density [kg/m^3]	950
Heat capacity [J/kg°C]	2300

selection of the optimum analysis method for the data obtained from the experiment.

There are many parameters to be considered in general. The orthogonal array table not only considers all parameters, but also excludes information about the interaction between parameters. As a result, the number of a numerical analysis or experiments can be minimized. We can also easily analyze the effect of parameters from the results.

2.4. Response surface method

RSM (response surface method) is a chain of processes that assumes a relation between the parameters and the response function as a mathematical equation, assumes a coefficient of the equation with the least squares method from results, and then makes a useful response surface model (Youn and Choi, 2004). In this study, a second response surface model is used as follows:

$$y = \beta_o + \sum_{i=1}^{n_d} \beta_i x_i + \sum_{i=1}^{n_d} \sum_{j \geq i}^{n_d} \beta_{ij} x_i x_j , \tag{6}$$

where x_i is the parameter, n_d is the number of the parameter and β_i is coefficient assumed by the least squares method.

Equation (7) is the calculation method of the coefficient of the response surface model.

$$\beta = (X^T X)^{-1} X^T Y , \tag{7}$$

where X is a parameter matrix composed of experimental points and Y is a response vector.

3. Geometry and process parameters

3.1. Shape of screw equipment

In this study, we considered the pitch as the shape parameter and the screw speed as the process parameter to investigate the mixing performance. We also modeled a single

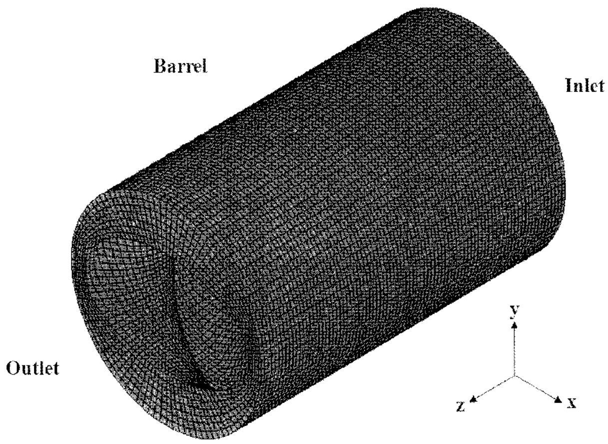

Fig. 2. Analysis domain of screw equipment.

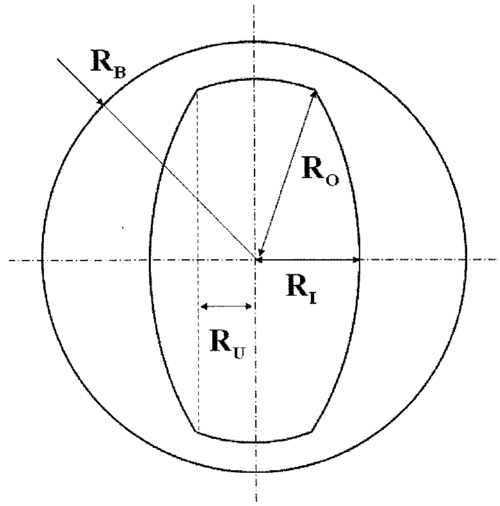

Fig. 3. Cross section of screw equipment.

Table 2. Screw extruder dimension

R_B	R_O	R_I	R_U
13 mm	11 mm	7 mm	3 mm

screw equipment as shown in Fig. 2. Symbols and dimensions of geometric parameters used in modeling of analysis domain are shown in Fig. 3 and Table 2, respectively.

3.2. Assumptions for numerical modeling

We assumed to analyze the flow characteristics as follows:

1) The flow in the screw extruder is laminar, because the velocity magnitude of the polymer melt is very slow due to the high viscosity characteristics of the polymer melt. As a result, Reynold's number of polymer melt is small in the screw equipment.

2) The viscosity is modeled as a function of temperature and deformation rate.

3) Heat generation was considered due to the viscous dissipation of the polymer melt.

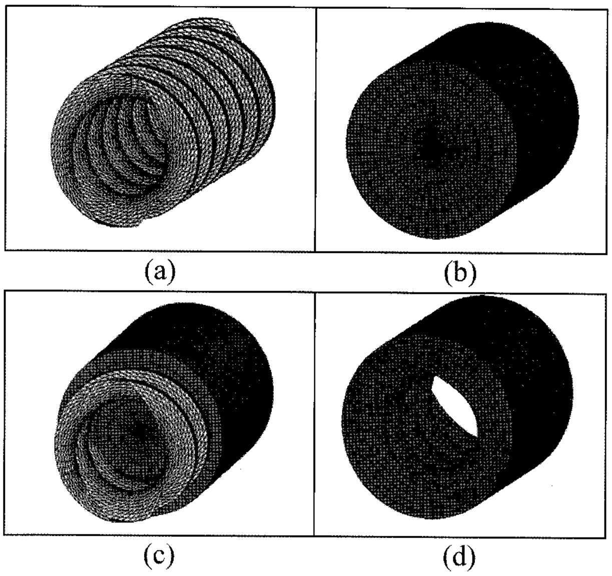

Fig. 4. Modeling procedural of analysis domain.

4) A thermal condition between the screw and polymer melt is adiabatic.
5) Properties of the polymer melt are constant values.
6) The barrel is fully filled with the polymer melt.
7) The polymer melt is an incompressible fluid.
8) A distance between inlet and outlet is 42 mm. In fact, the screw extruder is generally longer than this distance. However, this distance is sufficient to investigate the mixing performance in the screw equipment.

3.3. Boundary conditions

We applied boundary conditions for the flow analysis as follows:
1) No-slip boundary condition is applied on the solid surfaces of screw and barrel. In other words, the relative velocity between the polymer melt and solid is zero.
2) Barrel temperature is uniform overall as 200°C.
3) Temperature at inlet is constant to 190°C. On the other hand, thermal condition at outlet is dT/dz=0.
4) Relative pressure between inlet and outlet is set to be 0.1 MPa.

3.4. Modeling procedure of analysis domain

We modeled the analysis domain according to the following procedures as illustrated in Fig. 3:
1) The screw shape is modeled by using I-DEAS. This is transformed to shell element in STAR-CD as shown in Fig. 4(a).
2) The analysis domain is modeled as shown in Fig. 4(b).
3) The analysis domain and shell element overlap each other as shown in Fig. 4(c).
4) The analysis domain is projected to the shell element in the radial direction as shown in Fig. 4(d).

The number of control volumes is 268800, and it takes 10~12 hours computing time a case in SRAR-CD. Relaxation factor of convergence characteristics is 0.7.

4. Mixing performance indexes

The mixing performance is caused by the mechanical motion or shear force in polymer melt due to the screw extruder. In general, the mixing performance is divided into two categories: dispersive mixing and distributive mixing. Dispersive mixing means the degree that the particles in the polymer melt are broken down into pieces, while distributive mixing means the spatial distribution of the particle in the polymer melt. Dispersive mixing generally appears together with distributive mixing.

4.1. Deformation rate

As the dispersive mixing performance index, the magnitude of the rate-of-deformation tensor is expressed by equation (8). In general, it can be called shear deformation or deformation rate and be used as a dispersive mixing index. We call it as the deformation rate in this study.

$$|\dot{\gamma}(t)| = \left[\begin{array}{l} 2\left(\frac{\partial u}{\partial x}\right)^2 + 2\left(\frac{\partial v}{\partial y}\right)^2 + 2\left(\frac{\partial w}{\partial z}\right)^2 \\ + \left(\frac{\partial v}{\partial x} + \frac{\partial u}{\partial y}\right)^2 + \left(\frac{\partial w}{\partial y} + \frac{\partial v}{\partial z}\right)^2 + \left(\frac{\partial u}{\partial z} + \frac{\partial w}{\partial x}\right)^2 \end{array}\right]^{\frac{1}{2}} \tag{8}$$

4.2. Residual time distribution

As the distributive mixing performance index, the residence time distribution can be used as distributive mixing index. This index means the spatial distribution of the particles in the polymer melt. In this study, we calculated by using the particle tracking method based on the calculated velocity field. In other words, massless particles are numerically traced by calculating the spatial distribution of particles that move according to the velocity field. Second order Runge-Kutta numerical integration scheme is used to the particle tracking method. The residence time distribution is indicated as a cumulative distribution function as expressed in equation (9). This index means a ratio of particles that arrive at outlet.

$$F(t) = C_{out}(t)/C_{\infty}\,, \tag{9}$$

where, $C_{out}(t)$ is the number of the particles that arrive in outlet with respect to time, while C_{∞} is total number of particles.

F(t) becomes zero if time is zero. If time is infinite or if all particles arrive in outlet, F(t) becomes one. On the other hand, the slope of function cannot become negative (Kim *et al*, 2006a).

4.3. Total strain

The other mixing performance index is the total strain as expressed in equation (10). As a mixing performance

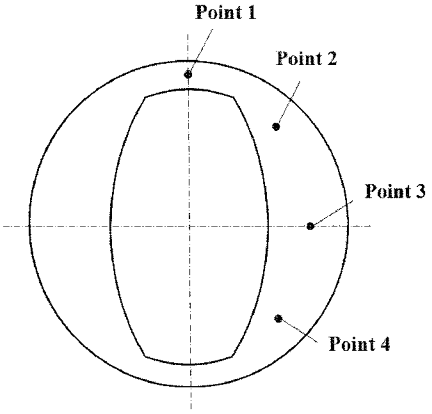

(a) Points for the particle tracking at the middle between inlet and outlet

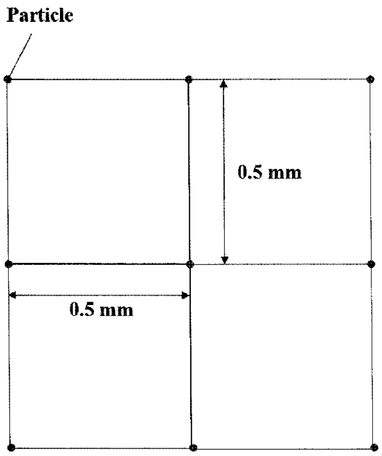

(b) Arrangement of the particles at the point

Fig. 5. Particle standard deviation.

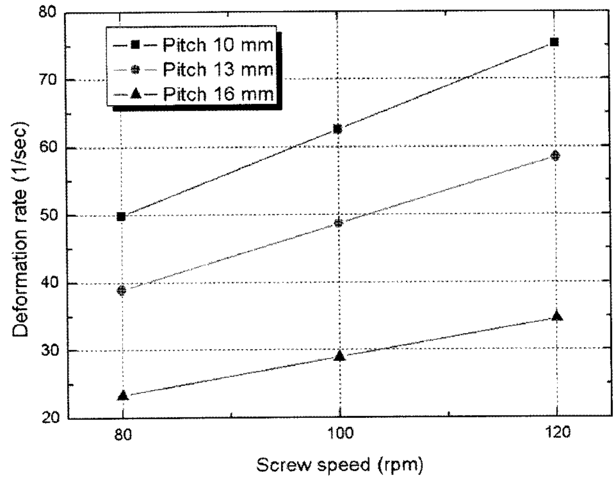

Fig. 6. Deformation rate with respect to the pitch and screw speed.

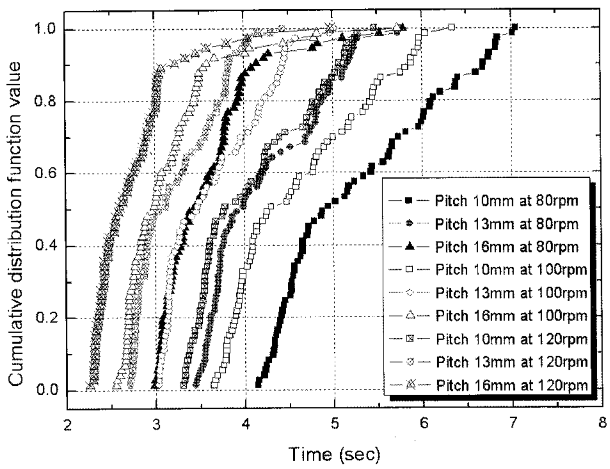

Fig. 7. Residence time distribution.

index, the total strain means the sum of the deformation rate in equation (8) during the residual time in equation (9). In other words, this index contains two mixing performance indexes: the deformation rate and residence time distribution.

$$\gamma(t) = \int_0^t \dot{\gamma}(t)dt \tag{10}$$

4.4. Particle standard deviation

As expressed in equation (11), we present PSD (particle standard deviation) as a new index for the mixing performance.

$$\sigma = \sqrt{\frac{\sum(x_{i,j}-m)^2}{n}} \tag{11}$$

where, $x_{i,j}$ is the coordinates of the particles that arrive at outlet after the particles are injected at the middle between inlet and outlet. m is an average value of these coordinates. And n is the number of the particles.

As shown in Fig. 5(a), we injected the particles into the polymer melt at Point 1, 2, 3 and 4 to obtain PSD in this study. On the basis of one point, total nine particles are injected at regular intervals of 0.5 mm.

4.5. Results and discussion

Fig. 6 shows the variation of the deformation at Point 1 in Fig. 5(a) with respect to the screw speed and pitch. The deformation rate increased as the increase of the screw speed or the decrease of the pitch. In the words, the mixing performance increased with the increase of the screw speed or with the decrease of the pitch on the basis of the deformation rate.

The residence time distribution as the other mixing performance index is shown in Fig. 7. We considered that some 140 particles are injected at regular intervals of 0.1 mm at the middle between inlet and outlet. Here, the cumulative distribution function '1' means that all particles arrive at outlet.

The cumulative distribution function decreased as the increase of the screw speed or pitch as shown in Fig. 7. The decrease of the residence time means that the particles

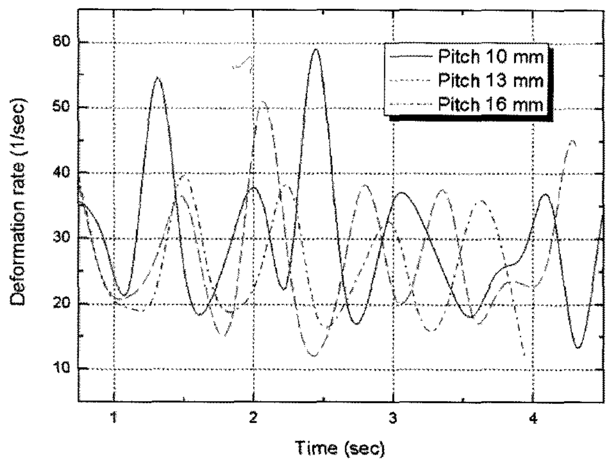

Fig. 8. Deformation rate with respect to the residence time.

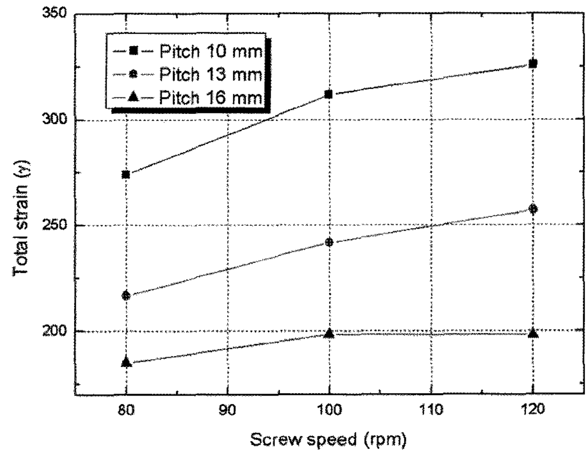

Fig. 10. Total strain with respect to the pitch and screw speed.

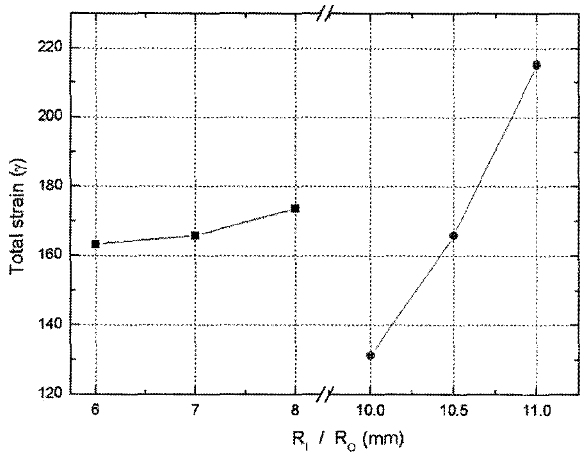

Fig. 9. Total strain with respect to the dimension of the screw.

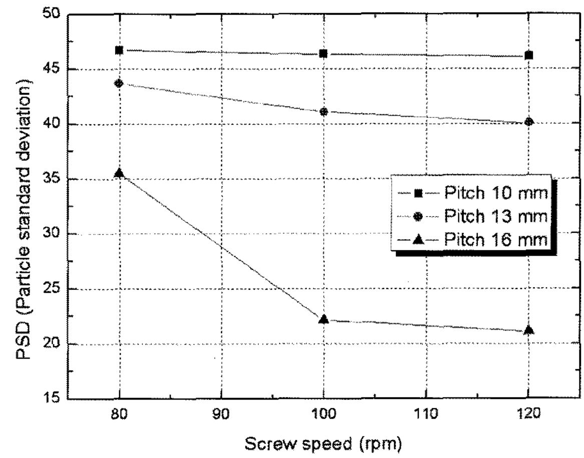

Fig. 11. PSD with respect to the pitch and screw speed.

stay in the screw extruder during a short period. Therefore, it means the decrease of the mixing performance. In conclusion, the residence time distribution increased with the decrease of the screw speed or pitch.

Fig. 8 shows the variation of the deformation rate with respect to the time and pitch when a particle is injected at Point 1 in Fig. 5(a). The deformation rate changed with respect to time. This reason is that the position of the particle in the screw extruder changed with respect to time. Furthermore, the deformation rate of the particle also changed with respect to time.

As a result, the total strain in equation (10) is the integral value of the deformation rate with respect to time. We used the trapezoidal rule to obtain the total strain in this study.

Fig. 9 shows the variation of the total strain with respect to R_O and R_I as shape parameters. The total strain increased as the increase of R_O or R_I. In particular, R_O has more influence than R_I on the total strain. The increase of R_O and R_I means the increase of the cross section of the screw. Therefore, the total strain increased with the increase of the cross section of the screw.

The total strain varied with respect to the screw speed and pitch as illustrated in Fig. 10. The total strain increased with the increase of the screw speed or the decrease of the pitch. On the basis of the deformation rate and residence time distribution, the deformation rate increased with the increase of the screw speed or the decrease of the pitch as shown in Fig. 6, like the total strain. On the other hand, the residence time distribution increased as the decrease of the screw speed or pitch as shown in Fig. 7. In other words, the increase of the screw speed caused the decrease of the residence time distribution. In conclusion, the rate of the increase of the total strain decreased as the increase of the screw speed. In particular, there is little difference of the total strain between screw speed 100 and 120rpm at pitch 16 mm.

Fig 11 shows the variation of PSD with respect to the screw speed and pitch. The decrease of PSD means that the particles are tightly clustered. On the other hand, the increase of PSD means that they are widely scattered. PSD increased as the decrease of the screw speed or pitch. In conclusion, the particles widely scattered with the decrease

Table 3. Level of design variables

Design variable	Level 1	Level 2	Level 3
R_O	10.0 mm	10.5 mm	11.0 mm
R_I	6.0 mm	7.0 mm	8.0 mm
R_U	2.5 mm	3.0 mm	3.5 mm
Pitch	10.0 mm	13.0 mm	16.0 mm
Scew speed	80.0 rpm	100.0 rpm	120.0 rpm

Table 4. Table of orthogonal arrays

No.	R_O	R_I	R_U	Pitch	Screw speed	Total strain	PSD
1	1	1	1	1	1	-274.6	-36.67
2	1	2	2	2	2	-262.6	-31.40
3	1	3	3	3	3	-200.1	-39.08
4	2	1	1	2	2	-256.4	-41.48
5	2	2	2	3	3	-265.5	-37.55
6	2	3	3	1	1	-429.8	-41.28
7	3	1	2	1	3	-702.6	-38.86
8	3	2	3	2	1	-430.7	-41.60
9	3	3	1	3	2	-338.7	-36.61
10	1	1	3	3	2	-177.7	-35.92
11	1	2	1	1	3	-350.5	-34.84
12	1	3	2	2	1	-229.9	-39.78
13	2	1	2	3	1	-219.5	-38.71
14	2	2	3	1	2	-436.2	-42.21
15	2	3	1	2	3	-364.8	-37.13
16	3	1	3	2	3	-513.6	-41.41
17	3	2	1	3	1	-260.9	-37.60
18	3	3	2	1	2	-607.1	-42.97

of the screw speed or pitch.

5. Design of experiments and response surface method

5.1. Orthogonal array

On the basis of each mixing performance, we considered five design parameters. The five design parameters consisted of the shape parameters (R_O, R_I, R_U and the pitch) and the process parameter (screw speed).

Each parameter is classified to 3 levels and Table 3 shows the values of the parameters with respect to their level. The composition of the table of the orthogonal array $L_{18}(3^5)$ is shown in Table 4. We considered the total strain as expressed in (10) and PSD as illustrated in (11) for the object functions in this study.

Table 5. Response surface method for total strain

Object function for total strain					
$\Phi = 36.294R_O^2+1.138R_I^2-8.31R_U^2$ $-0.292P^2+0.013S^2-822.273R_O-126.49R_I$ $+158.021R_U+28.433P-2.550S+8.253R_OR_I$ $+3.707R_IR_U-0.282R_IS+0.130R_IS$ $-2.754R_OR_U-6.173R_UP-0.248R_US$					
	R_O (mm)	R_I (mm)	R_U (mm)	Pitch (mm)	Screw speed (rpm)
Optimal design variable	13.0	9.0	2.1	10.0	200.0
Optimum value of total strain					
$-4245.0 \rightarrow -4436.0$					

5.2. Optimum values of mixing performance indexes

On the basis of the object functions in the orthogonal arrays, the optimal values of the total strain and PSD shown in Table 5 and 6. We used RSM for these optimal values. To obtain the optimal value of the object function, initial values of R_O, R_I, R_U, pitch and screw speed are 10.5 mm, 7.0 mm, 3.0 mm, 13.0 mm and 100.0 rpm, respectively. On the other hand, constrains of R_O, R_I, R_U, pitch and screw speed are 9.0~13.0 mm, 5.0~9.0 mm, 2.0~4.0 mm, 10.0~20.0 mm and 50.0~200.0 rpm, respectively.

As a result of RSM, the optimal values of the total strain and PSD are −4245.0 and −95.764, respectively. In the case of the total strain, the optimal design variables of R_O, R_I, R_U, pitch and screw speed are 13.0 mm, 9.0 mm, 2.1 mm, 10.0 mm and 200.0 rpm, respectively. On the other hand, in the case of PSD, the optimal design variables of R_O, R_I, R_U, pitch and screw speed are 10.4 mm, 9.0 mm, 2.0 mm, 10.0 mm and 72.2 rpm, respectively.

The reason of the difference between the optimal values of the total strain and PSD is as follows: the total strain increased with the increase of the screw speed. As a result, the total strain has the optimal value at the maximum screw speed, 200 rpm. On the other hand, PSD increased with the decrease of the screw speed. PSD does not have the opti-

Table 6. Response surface method for PSD

Object function for PSD					
$\Phi=-241.330R_O^2-31.471R_I^2+216.405R_U^2$ $+0.560P^2-0.095S^2 4713.052R_O+8.11977R_I$ $-3114.394R_U-16.735P+15.035S-26.190(R_OR_I)$ $+11.097R_IR_U-1.903R_IS-0.869R_IS$ $+111.507R_OR_U+19.064R_UP+2.445R_US$					
	R_O (mm)	R_I (mm)	R_U (mm)	Pitch (mm)	Screw speed (rpm)
Optimal design variable	10.4	9.0	2.0	10.0	72.2
Optimum value of PSD					
−95.76 → −90.88					

mal value at the minimum screw speed, 50 rpm. PSD has the optimal value at 72.2 rpm. This reason is why the others (R_O, R_I, R_U and pitch) have influence on these effect of the screw speed.

Finally, we carried out the flow analysis as the numerical analysis for the confirmation of these optimal values, which are obtained by using DOE and RSM. In this analysis, we design the screw extruder on the basis of the optimal design variables as shown in Table 5 and 6. As a result of the flow analysis, the difference between the optimal value of the total strain and numerical result is about 4.5%. And the difference between the optimal value of PSD and numerical result is about 5.1%. In conclusion, the optimal design methodology by using DOE and RSM in this study is a valid method to obtain the maximum mixing performance. This method can be used for not only the mixing performance of screw extruder but also for various other fields of study.

6. Conclusions

In this study, we carried out the flow analysis by using the commercial code, STAR-CD for FVM. Furthermore, we compared four mixing performance indexes: residence time distribution, deformation rate, total strain and PSD as a new mixing performance index in this study. To obtain the optimal value of the mixing performance, we considered the screw dimensions and screw speed as the design parameters. To obtain the optimal values of the total strain and PSD, we used the response surface method and design of experiments.

From the results, we obtained the following conclusions:

1) As the dispersive mixing performance index, the deformation rate increased with the increase of the screw speed or the decrease of the pitch.

2) As the distributive mixing performance index, the residence time distribution increased with decrease of the pitch. However, contrary to the deformation, it decreased as the increase of the screw speed.

As a mixing performance index contains the deformation rate and residence time distribution, the total strain increased with the increase of the screw speed or the decrease of the pitch. However, the increase rate of the total strain decreased with the increase of the screw speed due to the decrease of the residence time.

The total strain also increased with the increase of R_O or R_I as the shape parameters.

PSD increased as the decrease of the screw speed or pitch. It means that the particles are widely scattered with the decrease of the screw speed or pitch.

The differences between the optimal values and numerical results are about 5.0%.

Nomenclatures

t	: Time
x_j	: Cartesian coordinate ($j=1,2,3$)
u_j	: Velocity component in the x_j-direction
u, v, w	: Velocity components in the x-, y-, z-directions, respectively
$x_{i,j}$	: Cartesian coordinate of the particles in PSD
p	: Pressure
T	: Temperature
T_o	: Reference temperature
s_m	: Mass source term
s_i	: Momentum source term
s_h	: Energy source term
h	: Enthalpy
$F_{h,j}$	: Diffusional energy flux in the x j-direction
s_{ij}	: Strain rate tenser
a_T	: Temperature shift factor
k_i	: Constants in Bird-Carreau-Yasuda model
E_o	: Activation energy
R	: Gas constant
m	: Average value of the coordinates in PSD
n	: The number of the particles in PSD
x_i	: Parameters
n_d	: The number of the parameter
X	: Parameter matrix
Y	: Response vector

Greek symbols

ρ	: Density
τ_{ij}	: Stress tensor components
μ	: Viscosity
$\dot{\gamma}$	: Deformation rate
δ_{ij}	: Kronecker delta
β	: Coefficient of the response surface model

References

Bakalis, S. and M. V. Karwe, 2002, Velocity distributions and volume flow rates in the nip and translational regions of a co-rotating, self-wiping, twin-screw extruder, *Journal of Food Eng.* **51**, 273-282.

Bravo, V. L. and A. N. Hrymak, 2000, Numerical Simulation of Pressure and Velocity Profiles in Kneading Elements of a Co-Rotating Twin Screw Extruder, *Polymer Eng. and Sci.* **40(2)**, 525-541.

Bravo, V. L., A. N. Hrymak and J. D. Wricht, 2004, Study of Particel Trahectories, Residence Times and Flow Behavior in Kneading Discs of Intermeching Co-Rotating Twin-Screw Extruders, *Polymer Eng. and Sci.* **44(4)**, 779-793.

Fenner, R. T., 1977, Development in the analysis of steady screw extrusion of polymers, *Polymer* **18**, 617-635.

Griffith, R. M., 1962, Fully developed flow in screw extruder, *Ind. Eng. Chem. Fundam.* **1**, 180-187.

Ishikawa, T., S. I. Kihara and K. Funatsu, 2000, 3-D Numerical Simulations of Non-isothermal Flow in Co-Rotating Twin Screw Extruders, *Polymer Eng. and Sci.* **40(2)**, 357-364.

Ishikawa, T. and T. Amano, 2002, Flow Pattern and Mixing Mechanisms in the Screw Mixing Element of a Co-Rotating Twin-Screw Extruder, *Polymer Eng. and Sci.* **42(5)**, 925-939.

Karwe, M. V. and T. Jaluria, 1990, Numerical simulation of fluid flow and heat transfer in a single screw extruder for non-Newtonian fluids, *Numerical heat transfer*, Part A: Application **17**, 167-190.

Khalifeh, A. and J. Clermont, 2005, Numerical Simulation of Non-isothermal Three-Dimensional Flows in an Extruder by a Finite Volume Method, *J. Non-Newtonian Fluid Mech.* **126**, 7-22.

Kim, N. S., H. B. Hong and J. W. Lee, 2006, Numerical analysis of internal flow and mixing performance in polymer extruder I: single screw element, *Korea-Australia Rheology Jol.* **18(3)**, 143-151.

Kim, N. S., H. B. Hong and J. W. Lee, 2006, Numerical analysis of internal flow and mixing performance in polymer extruder II: twin screw element, *Korea-Australia Rheology Jol.* **18(3)**, 153-160.

Kim, S. J. and T. H. Kwon, 1996a, Enhancement of mixing performance of single-screw extrusion processes via chaotic flows: Part I, Basic concepts and experimental study, *Advances in Ploymer Tech.* **15**, 41.

Kim, S. J. and T. H. Kwon, 1996b, Enhancement of mixing performance of single-screw extrusion processes via chaotic flows: Part II, Numerical study, *Advances in Ploymer Tech.* **15**, 55.

Kwag, D. S., W. S. Kim, K. S. Lee and M. Y. Lyu, 2001, A three-dimensional numerical study of fluid flow and heat transfer in the single screw extruder, *Proceeding of the second International Conference on Computational Heat and Mass Transfer* 22-26.

Kwon, T. H., J. W. Joo and S. J. Kim, 1993, Kinematics and deformation characteristics as a mixing measure in the screw extrusion process, *Polymer Eng. and Sci.* **34**, 174-189.

Lim, J. M., S. Han, S. Jeon, D. Woo and G. J. Park, 1999, Analysis and Design Considerations of Energy Absorbing Steering System using Orthogonal Arrays, *Trans. KSAE* **7(6)**, 144-155.

Linjie, Z., A. N. Kwabena, and S. H. Kun, Investigation of Mixing mechanisms and energy balance in reactive extrusion using three-dimensional numerical simulation method, 2005, *International Journal of Heat and Mass Transfer* **48**, 3411-3422.

Osswald, T. A. and G. Menges, Material Science of Polymers for Engineers 2nd ed., 2007, *Hanser Gardner Pubns.* 129-147.

Osswald, T. A. and J. P. Hernandez-Ortiz, Polymer Processing; Modeling and Simulation, 2006, *Hanser Gardner Pubns* 68-74

Sastrohartono, T., Y. Jaluria, M. Esseghir and V. Sernas, 1994, A numerical and experimental study of three-dimensional transport in the channel of an extruder for polymeric materials, *Int. J. Heat Mass Transfer* **38(11)**, 1957-1973.

Shearer, G. and C. Tzoganakis, 2000, The Effects of Kneading Block Design and Operating Conditions of Distributive Mixing in Twin Screw Extruders, *Polymer Eng. and Sci.* **40(5)**, 1095-1106.

Syrjala, S., 1999, On the Analysis of Fluid Flow and Heat Transfer in the Melt Conveying Section of a Single Screw Extruder, *Numerical Heat Transfer*, Part A **35**, 25-47.

Syrjala, S., 2000, Numerical Simulation of Non-isothermal Flow of Polymer Melt in a Single Screw Extruder: A Validation Study, *Numerical Heat Transfer*, Part A **37**, 897-915.

Ye, Y. S., H. B. Kim, N. Kim, and J. W. Lee, 2005, A Study on Analysis of Polymer Extruder Process using Finite Element Method, *The Korean Society of Mechanical Engineers Part A* **29(1)**, 145-155.

Youn, B.D. and K.K. Choi, 2004, A new Response Surface Methodology for Reliability Based Design Optimization, *Computers and Structures* **82**, 241-256.

Yoshinaga, M., S. Katsuki, M. Miyazaki, L. Liu, S. I. Kihara, and K. Funatsu, 2000, Mixing Mechanism of Three-Tip Kneading Block in Twin Screw Extruders, Polymer Eng. and Sci. **40(1)**, 168-178.